

Shakeoff Ionization near the Coulomb Barrier Energy

Prashant Sharma* and T. Nandi†

Inter-University Accelerator Centre, Aruna Asaf Ali Marg, New Delhi 110067, India

(Received 14 June 2017; revised manuscript received 31 July 2017; published 13 November 2017)

We measure the projectile K x-ray spectra as a function of the beam energies around the Coulomb barrier in different collision systems. The energy is scanned in small steps around the barrier aiming to explore the nuclear effects on the elastically scattered projectile ions. The variation of the projectile x-ray energy with the ion-beam energies exhibits an unusual increase in between the interaction barrier and fusion barrier energies. This additional contribution to the projectile ionization can be attributed to the shakeoff of outer-shell electrons of the projectile ions due to the sudden nuclear recoil ($\sim 10^{-21}$ sec) caused by the attractive nuclear potential, which gets switched on near the interaction barrier energy. In the sudden approximation limit, the theoretical shakeoff probability calculation due to the nuclear recoil explains the observed data well. In addition to its fundamental interest, such processes can play a significant role in dark matter detection through the possible mechanism of x-ray emissions, where the weakly interacting massive particle-nucleus elastic scattering can lead to the nuclear-recoil-induced inner-shell vacancy creations. Furthermore, the present work may provide new prospects for atomic physics research at barrier energies as well as provide a novel technique to perform barrier distribution studies for two-body systems.

DOI: [10.1103/PhysRevLett.119.203401](https://doi.org/10.1103/PhysRevLett.119.203401)

The well-known disparity between the interaction range and coupling constant for the electromagnetic and strong force suggests an independent treatment of atomic and nuclear phenomena. However, some distinct processes, viz., bound-state β decay [1], nuclear excitation by electron capture [2], etc., occurring at the borderline between atomic and nuclear physics, provide a possibility to explore the interference between such interactions. Similarly, the Coulomb barrier region also may provide an opportunity to study the interplay between atomic and nuclear processes [3]. Nevertheless, no effort has been invested yet in studying the influence of the nuclear interaction on the atomic processes at barrier energies during ion-atom collisions. In order to investigate the nuclear influence on the atomic processes, we have recorded the projectile ion K x-ray spectra as a function of the beam energies around the barrier. With great surprise, we observe an unusual increase or a kink in the gradual variation of x-ray energy as the beam energy approaches to the Coulomb barrier regime. Noteworthy, when the swift projectile ions pass through a solid target, the electron loss and capture processes are the primary phenomena. These processes mainly depend on electron-nucleus and electron-electron correlation and generally exist at every beam energy. However, the influence of nuclear-nuclear interaction on the electronic environment can be exhibited only if the two collision partners come close to the short nuclear ranges. Hence, the nuclear interaction can be a possible effect for such a kink.

In this Letter, the underlying physical origin is explained in terms of the shakeoff ionization caused by the sudden recoil of projectile ions [4,5] as they encounter the barrier potential. This finding has been validated with three

different systems, viz. $^{12}\text{C}(^{56}\text{Fe}, ^{56}\text{Fe})$, $^{12}\text{C}(^{58}\text{Ni}, ^{58}\text{Ni})$, and $^{12}\text{C}(^{63}\text{Cu}, ^{63}\text{Cu})$. Interestingly, the ionization and excitation of bound atomic electrons of detector material can also be induced by the elastic recoiling of the atomic nucleus with the impact of the weakly interacting massive particles (WIMPs), which may result in characteristic x-ray emissions to provide excellent opportunities to detect sub-GeV WIMPs [6,7]. Therefore, the present work may complement earlier theoretical works [4,5] and has implications in the dark-matter search experiments [6,7].

Three experimental runs were carried out using the 15 UD tandem [8]. Ion beams of ^{56}Fe , ^{58}Ni , and ^{63}Cu (current = 1–2 pA) at several beam energies covering the Coulomb barrier region in small steps were passed through carbon foil. The foil thickness was $80\text{ }\mu\text{g}/\text{cm}^2$ for the ^{56}Fe and ^{58}Ni experiments and $60\text{ }\mu\text{g}/\text{cm}^2$ for the ^{63}Cu experiment. To avoid any deterioration effect due to ion-solid collisions, the target with similar thickness was replaced in each experimental run. The pressure around 1×10^{-6} Torr was maintained in the experimental chamber.

During the passage of projectile ions through the bulk of the target, various charge-changing processes including ionization, excitation, electron capture, etc., lead to a certain distribution of the projectile charge states. After a large number of collisions, the projectile ions attain an equilibrium charge state distribution (CSD), and the corresponding target thickness is called equilibrium thickness. However, the electron capture processes occurring at the exit of the target surface greatly influence the projectile charge state attained in the bulk. Conventional electromagnetic methods measure the total charge state of the ions and,

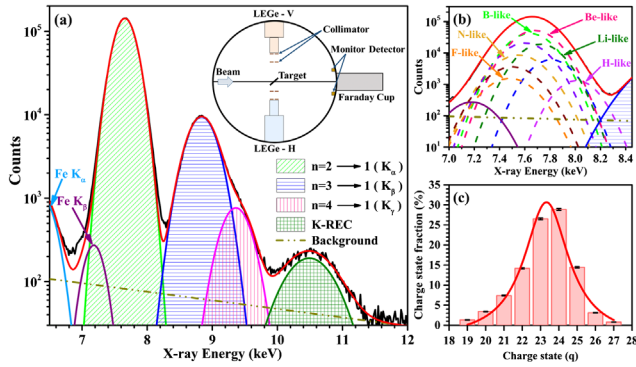


FIG. 1. Systematics of the analysis for a typical case of the 120 MeV $^{58}\text{Ni}^{12+}$ beam on $80 \mu\text{g}/\text{cm}^2$ ($\sim 113 \mu\text{g}/\text{cm}^2$ at 45°) carbon foil: (a) x-ray spectrum showing the projectile x rays corresponding to K_α , K_β , K_γ , and K -REC peaks. The Fe K_α and K_β peaks due to the beam halo hitting the target frame are also shown. A schematic of the setup is shown in the inset. (b) Deconvolution of the K_α x-ray peak corresponding to different charge states (H-like to F-like). (c) CSD calculated using Eq. (1). The raw x-ray spectra, observed at different beam energies are shown in Supplemental Material [14].

therefore, cannot determine the actual CSD occurring in the bulk only [9]. In the present work, we have used the characteristic x-ray emissions to determine the projectile CSD [9] as employed in other fields [10,11].

Two germanium ultralow-energy detectors (GUL0055 and GUL0035, Canberra Inc., with a $25 \mu\text{m}$ thick Be entrance window, resolution 150 eV at 5.9 keV, and constant detector efficiency in the range of 5–20 keV) were placed at $\pm 90^\circ$ to the beam axis as shown in the inset of Fig. 1(a). The x rays enter the detectors through the thin Mylar windows of $6 \mu\text{m}$. This geometry of the detectors covers the ion-solid collision zone through the back and front surfaces of the foil. The collimating system of suitable sizes was placed in front of the detectors to ensure the probing of the ion-solid collision zone only. For this geometry, the Doppler broadening is maximum, but the first-order Doppler shift is zero and the second-order shift appears at the fourth or fifth decimal place depending on the beam energies. Hence, the x-ray energy peaks do not require any further corrections. The measured spectra from both the detectors were alike and followed the same trend. It is noteworthy that the target foil holder has been put at 45° to the beam axis for recording the prompt x-ray spectra emanating right from the collision zone. At this orientation, the target thickness used turns out to be about twice the theoretical equilibrium thickness at the highest beam energy [12]. Hence, a charge equilibrium is most likely attained for all the beam energies [13]. To check the systematic errors, the observed x-ray spectra, collected from both the detectors, were calibrated with different radioactive sources like ^{55}Fe , ^{57}Co , and ^{241}Am before as well as after the experiments and no significant deviations were found. Furthermore, the calibrations were also

supervised during the online data collection through observing the Fe K_α and Fe K_β peaks due to the beam halo hitting the foil holder made of stainless steel in the case of ^{58}Ni and ^{63}Cu projectile ions. However, for the Fe-beam experiment, the beam was passed through a blank target frame to minimize the halo and its effect on the peak structure originating from the projectile ions.

A typical x-ray spectrum consisting of characteristic transitions (K_α , K_β , and K_γ) and a radiative electron capture (REC) peak for the ^{58}Ni projectile ions passing through the carbon foil at 120 MeV is shown in Fig. 1(a) with different patterns and colors. As the ion passes through the foil, several charge states are evolved due to the multiple vacancy creations in both the atomic systems. These vacancies decay subsequently through various rearrangement processes leading to the characteristic x-ray emissions. Since the x-ray detectors used in the experiments cannot resolve the x-ray emissions from the individual projectile charge states, each peak represents a convolution of different x-ray lines [Fig. 1(b)], and its centroid denotes the x-ray transition energy of the mean charge state (q_m) [9]. With increasing collision energy, multiple vacancy creations in projectile ions increase, which results in the enhancement of the relative fraction of higher charge state ions compare to lower charge state ions. As a consequence, the centroid of the convoluted projectile x-ray peak shifts gradually towards the higher x-ray energy side, as evident in Fig. 2, where the variations of the K_α and K_β x-ray energies are portrayed as a function of the beam energies. The fitting error in the centroid energy is found to be less than 1% and smeared in the symbol size except for the ^{63}Cu K_β curve [Fig. 2(c')]. The x-ray energy increases monotonically with variation in the third decimal place up to a certain point, and then it jumps suddenly to the second decimal place. This feature can be amplified in the derivative curve as depicted in Figs. 2(a)–2(c) and 2(a')–2(c'), where the curves display sudden jumps at 119.75 ± 0.62 , 133.95 ± 0.32 , and 142.56 ± 0.43 MeV for the experiments with ^{56}Fe , ^{58}Ni , and ^{63}Cu beams, respectively. Note that these values are in between the theoretical interaction barrier and fusion barrier energies of the corresponding two-body systems [15] as given in Table I.

Worth noting, the interaction barrier energy (E_b), unlike the fusion barrier energy (E_f) required by the participating nuclei to be within touching distance ($\approx R_1 + R_2$, where $R = 1.2 \times A^{1/3}$ fm and R and A are the nuclear radius and mass number, respectively), describes the minimum kinetic energy needed by the participating nuclei to undergo a dynamic quasielastic nuclear-nuclear interaction. It is the actual distance where the two nuclei start influencing each other. These facts can readily be seen in Figs. 2(a'')–2(c''), where the kink occurs far from touching distance and near the interaction barrier energy. It implies that K x-ray emissions are altered in the nuclear length scale, as observed

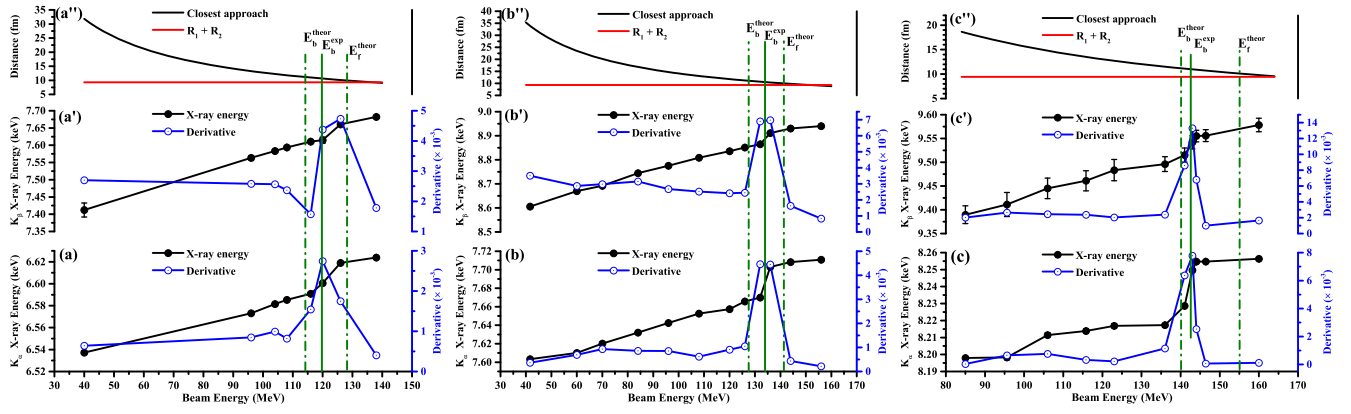


FIG. 2. Variation of projectile characteristic x-ray energy versus beam energy: (a) ^{56}Fe K_α , (a') ^{56}Fe K_β , (b) ^{58}Ni K_α , (b') ^{58}Ni K_β , (c) ^{63}Cu K_α , and (c') ^{63}Cu K_β . Error bars are tiny and smeared in the symbol size except the ^{63}Cu K_β curve. All solid lines are to guide the eye only. The dash-dot vertical lines represent the theoretical interaction barrier (E_b^{theor}) and theoretical fusion barrier (E_f^{theor}) of the corresponding systems [15], whereas the solid vertical line corresponds to the measured interaction barrier (E_b^{exp}). The values of E_f^{theor} , E_b^{theor} , and E_b^{exp} for each system are given in Table I. The distance of closest approach versus beam energy for the systems (a'') ^{56}Fe on ^{12}C , (b'') ^{58}Ni on ^{12}C , and (c'') ^{63}Cu on ^{12}C are also shown.

in an earlier study [16], which shows that the K -shell excitation probability is significant and narrowly peaked around the interaction barrier position. Therefore, the present method can be the simpler alternative for barrier distribution studies [17], which have paramount importance in probing both the static and dynamical properties of atomic nuclei during heavy-ion fusion reactions [18] and quasi-elastic nuclear reactions [19].

To verify whether any atomic processes are involved in the unusual ionization so observed, we examine the variation of q_m with the beam energy using the available theories. The mean charge states are measured by segregating the individual x-ray intensity with respect to different charge states using the x-ray spectroscopy method [9]. By fixing the centroid of the peaks to F-like to H-like projectile K_α x-ray energies, the convoluted x-ray peak is fitted with the different Gaussian functions corresponding to each charge state, as shown in Fig. 1(b). The overall fit has been ensured through varying the full width half maxima and intensities until the condition of least residuals achieved. The K_α x-ray energies of various ionic states of the respective projectile ions are obtained from the NIST

database [20] and multiconfiguration Dirac-Fock method using the GRASP-2K code [21]. Thus, we have measured the distribution of charge state fractions (CSFs) directly from the measured distribution of x-ray intensities as follows:

$$\text{CSF} = \frac{I_q/(\omega_q \epsilon_d)}{\sum_q I_q/(\omega_q \epsilon_d)} = \frac{I_q/\omega_q}{\sum_q I_q/\omega_q}, \quad (1)$$

where I_q and ω_q represent the x-ray intensity and fluorescence yield of the projectile ion for the particular charge state (q), respectively, whereas ϵ_d corresponds to the detector efficiency (constant). Furthermore, the fluorescence yield data for different projectile charge states were taken from Hasoğlu [22,23]. Subsequently, the mean charge states are calculated from the Lorentzian fitting of measured CSFs as shown in Fig. 1(c), and their uncertainties are simply the fitting errors. The measured mean charge states are compared with the semiempirical formalism [24] as well as theoretical code, ETACHA [12], in Fig. 3. Both the predictions are smoothly varying functions and thus unable to explain the unusual kink seen in the present experiments. Similar behavior is also evident in the only available measured charge state data for ^{63}Cu on ^{12}C [25], which exhibits the incapability of electromagnetic methods in probing such ionization process.

As discussed, Figs. 2(a)–2(c) and 2(a')–2(c') exhibit a sudden enhancement in projectile ionization as soon as the projectile ions approach the nuclear-nuclear interaction regime. At such short distances, the projectile and target nuclei no longer only repel due to the Coulomb interaction but rather attract also momentarily due to the strong interaction for the nuclear time scale of the order of

TABLE I. Comparison between the measured interaction barrier (E_b^{exp}) and theoretically estimated interaction barrier (E_b^{theor}) from the Bass model [15]. The predicted fusion barrier (E_f^{theor}) is also given for comparison [15].

System	E_f^{theor}	E_b^{theor}	E_b^{exp}
^{56}Fe on ^{12}C	128.16 MeV	114.16 MeV	119.75 ± 0.62 MeV
^{58}Ni on ^{12}C	141.38 MeV	127.54 MeV	133.95 ± 0.32 MeV
^{63}Cu on ^{12}C	155.06 MeV	140.12 MeV	142.56 ± 0.43 MeV

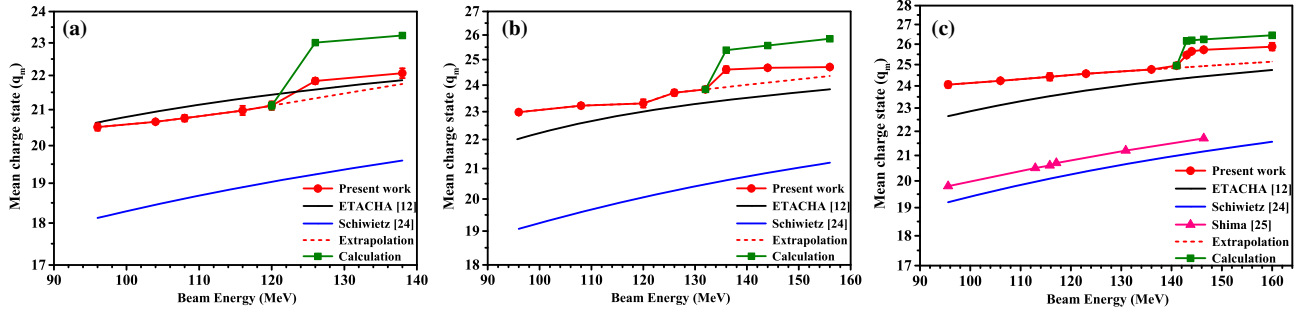


FIG. 3. Variation of mean charge state versus beam energy: (a) ^{56}Fe , (b) ^{58}Ni , and (c) ^{63}Cu beam on the carbon foil. Solid lines are to guide the eye only. Uncertainties are almost covered within the symbol size. See the text for other details.

10^{-21} sec. In contrast, the atomic time scale is large, of the order of 10^{-18} sec. Consequently, the nucleus of the projectile ion having a K vacancy can experience the resultant of the electromagnetic and strong interaction as a sudden recoil before decaying through the K x-ray emissions. For the present case, the projectile ions must be affected by the interaction barrier potential all of a sudden, which results in the nuclear recoil leading to the shakeoff ionization of outer electrons, i.e., L -shell electrons. The shakeoff probability under such a sudden perturbation can be evaluated as

$$W_{\text{so}} = \int_0^\infty |\langle \psi_\infty | \exp(i\vec{k} \cdot \vec{r}) | \psi_i \rangle|^2 dE, \quad (2)$$

where ψ_i is the hydrogenic electron wave function in the initial bound state, whereas ψ_∞ is the final hydrogenic continuum wave function of the electron with kinetic energy between E and $E + dE$ in the final recoiled state of the corresponding atomic system. k is the wave vector of the final system and given as

$$k = \frac{m_e}{M + Zm_e} \frac{p}{\hbar}, \quad (3)$$

where p ($= \sqrt{2ME_R}$, E_R is the recoil energy) represents the momentum of the recoiled nucleus in the center of mass frame, m_e is the electron mass, and M and Z are the mass and atomic number of the projectile ion, respectively.

Near the interaction barrier energy, the recoil energy of projectile nucleus may vary within two limiting conditions: (i) it is zero for large impact parameters and does not contribute to the shakeoff, and (ii) it is maximum (E_b^{exp}) for zero impact parameter and maximum change (Δq_{SO}) occurs with the q_m as follows:

$$\Delta q_{\text{SO}} = q_m \sum_{nlm} (N_{nlm} W_{nlm}) \frac{E_b^{\text{exp}}}{M}, \quad (4)$$

where N_{nlm} is the total number of electrons in the particular subshell. $W_{nlm} E_b^{\text{exp}}/M$ represents the electronic shakeoff

probability, where E_b^{exp}/M is in MeV/u, calculated using Eq. (2). The values of W_{nlm} are given in Table II. The symbols n , l , and m are the principle, orbital, and magnetic quantum number, respectively.

For the large impact parameter case, the projectile mean charge state (q_m) is due to Coulomb ionization, which can be deduced by extrapolating the measured, smoothly varying charge state versus the beam energy curve, as shown by the red dotted line in Fig. 3. Whereas, for the zero impact parameter case, the projectile mean charge state near E_b^{exp} can be defined as $q_m + \Delta q_{\text{SO}}$ and is depicted by the green line in Fig. 3. The changes in q_m due to the shakeoff for all three systems at various beam energies are compared with the measured ones in Figs. 3(a)–(c). As expected, the variation of measured mean charge states lies between two limiting cases (red dotted and green lines in Fig. 3), as mentioned above, and follows the same trend as the theoretically calculated values. The recoil-induced shakeoff processes may have potential importance in dark matter search experiments, where the WIMP-nucleus short-range interaction creates a sudden nuclear recoil in the target material. It can subsequently result in the creation of additional vacancies in the target atom, which decay through various rearrangement processes leading to characteristic x-ray production and electron emission. As noted in recent studies [6,7,26], these channels may be advantageous in the search for sub-GeV WIMPs detection. However, no detailed investigation of shakeoff processes exists in the field yet. We believe that, besides the new direction in the cross-link of atomic and nuclear physics, the present work might provide some new insights and scope for future dark matter search experiments.

TABLE II. Values of W_{nlm} for different L subshells ($2s$, $2p_z$, and $2p_{x,y}$) electrons of various projectile ions.

System	W_{200} ($2s$)	W_{210} ($2p_z$)	$W_{21\pm 1}$ ($2p_{x,y}$)
^{56}Fe on ^{12}C	0.0491	0.0402	0.0274
^{58}Ni on ^{12}C	0.0423	0.0346	0.0236
^{63}Cu on ^{12}C	0.0395	0.0323	0.0221

In conclusion, experiments performed with projectile K x rays have revealed an unusual enhancement in the ionization with the projectile ions approaching the nuclear interaction region during the passage through a thin carbon foil. The appearance of such an increase does not correspond to any usual charge changing processes. The unexpected increase in ionization near the interaction barrier is attributed to the influence of the resultant of the strong and electromagnetic force. It gives rise to the sudden recoil in the projectile nuclei that leads to the shakeoff ionization of the L -shell electrons of the projectile ions, which in turn provides the sudden change in the charge state of the projectile ions at the interaction barrier energy. The theoretical calculations corroborate the fact that the sudden shakeoff ionization process due to the nuclear recoil is responsible for the kink observed in the variation of projectile ionization as a function of beam energies. This study provides an exciting opportunity to advance our knowledge of charge-changing processes near the barriers, whereas in the nuclear physics front, the technique is evolved as a new method to measure the interaction barrier of two-body systems. Importantly, the present work draws attention to the significance of considering the shakeoff ionization as a possible mechanism for production of x rays during WIMP-nucleus scattering.

We acknowledge cooperation from the Pelletron accelerator staff and the colleagues of Atomic Physics group, IUAC, during the experiments. We also thank M. F. Hasoğlu gratefully for providing the theoretical fluorescence yield data. It is also our pleasure to thank A. Ray, P. Kumar, C. S. Unnikrishnan, A. Chatterjee, S. Kailas, H. S. Nataraj, Shreya Nandi, H. G. Berry, R. K. Bhowmik, A. K. Jain, T. Mukoyama, and G. W. F. Drake for illuminating discussions. P. S. is thankful to UGC, India for providing the financial support.

*phyprashant@gmail.com

†nanditapan@gmail.com

- [1] J. N. Bahcall, *Phys. Rev.* **124**, 495 (1961).
- [2] A. Pálffy, W. Scheid, and Z. Harman, *Phys. Rev. A* **73**, 012715 (2006).
- [3] M. S. Freedman, *Annu. Rev. Nucl. Sci.* **24**, 209 (1974).
- [4] A. B. Migdal, *Qualitative Methods in Quantum theory* (Benjamin, London, 1977), pp. 102–111.
- [5] L. Vegh, *J. Phys. B* **16**, 4175 (1983).
- [6] H. Ejiri, C. C. Moustakidis, and J. D. Vergados, *Phys. Lett. B* **639**, 218 (2006).
- [7] R. Bernabei, P. Belli, F. Montecchia, F. Nozzoli, F. Cappella, A. Incicchitti, D. Prosperi, R. Cerulli, C. J. Dai, H. L. He, H. H. Kuang, J. M. Ma, X. D. Sheng, and Z. P. Ye, *Int. J. Mod. Phys. A* **22**, 3155 (2007).
- [8] D. Kanjilal, S. Chopra, M. M. Narayanan, I. S. Iyer, V. Jha, R. Joshi, and S. K. Datta, *Nucl. Instrum. Methods Phys. Res., Sect. A* **328**, 97 (1993).
- [9] P. Sharma and T. Nandi, *Phys. Lett. A* **380**, 182 (2016).
- [10] J. T. Schmelz and J. C. Brown, *The Sun: A Laboratory for Astrophysics* (Library of Congress Cataloging-in-Publication Data, Washington, DC, 1991), pp. 261–276.
- [11] J. P. Santos, A. M. Costa, J. P. Marques, M. C. Martins, P. Indelicato, and F. Parente, *Phys. Rev. A* **82**, 062516 (2010).
- [12] J. P. Rozet, C. Stéphan, and D. Vernhet, *Nucl. Instrum. Methods Phys. Res., Sect. B* **107**, 67 (1996).
- [13] M. Imai, M. Sataka, K. Kawatsura, K. Takahiro, K. Komaki, H. Shibata, H. Sugai, and K. Nishio, *Nucl. Instrum. Methods Phys. Res., Sect. B* **267**, 2675 (2009).
- [14] See Supplemental Material at <http://link.aps.org/supplemental/10.1103/PhysRevLett.119.203401> for x-ray spectra at different beam energies for three systems, viz., $^{12}\text{C}(^{56}\text{Fe}, ^{56}\text{Fe})$, $^{12}\text{C}(^{58}\text{Ni}, ^{58}\text{Ni})$, and $^{12}\text{C}(^{63}\text{Cu}, ^{63}\text{Cu})$.
- [15] R. Bass, *Nucl. Phys. A* **231**, 45 (1974).
- [16] J. S. Greenberg, H. Bokemeyer, H. Emling, E. Grosse, D. Schwalm, and F. Bosch, *Phys. Rev. Lett.* **39**, 1404 (1977).
- [17] M. Dasgupta, D. J. Hinde, N. Rowley, and A. M. Stefanini, *Annu. Rev. Nucl. Part. Sci.* **48**, 401 (1998).
- [18] B. B. Back, H. Esbensen, C. L. Jiang, and K. E. Rehm, *Rev. Mod. Phys.* **86**, 317 (2014).
- [19] S. Mitsuoka, H. Ikezoe, K. Nishio, K. Tsuruta, S. C. Jeong, and Y. Watanabe, *Phys. Rev. Lett.* **99**, 182701 (2007).
- [20] Y. Ralchenko, A. E. Kramida, J. Reader, and N. Team, NIST Atomic Spectra Database (version 5.2), <http://physics.nist.gov/asd>, National Institute of Standards and Technology, Gaithersburg, MD, 2014.
- [21] P. Jönsson, X. He, C. Froese Fischer, and I. P. Grant, *Comput. Phys. Commun.* **177**, 597 (2007).
- [22] M. F. Hasoglu, Ph. D. thesis, Western Michigan University, 2008.
- [23] M. F. Hasoglu (private communication).
- [24] G. Schiwietz and P. L. Grande, *Nucl. Instrum. Methods Phys. Res., Sect. B* **175–177**, 125 (2001).
- [25] K. Shima, T. Mikumo, and H. Tawara, *At. Data Nucl. Data Tables* **34**, 357 (1986).
- [26] T. M. Undagoitia and L. Rauch, *J. Phys. G* **43**, 013001 (2016).